Decision-related pupil dilation reflects upcoming choice and individual bias

Jan Willem de Gee[a], Tomas Knapen[a,b], and Tobias H. Donner[a,c,d,1]

[a]Brain and Cognition, Department of Psychology, University of Amsterdam, 1018 XA, Amsterdam, The Netherlands; [b]Department of Psychology, Vrije Universiteit Amsterdam, 1018 WS, Amsterdam, The Netherlands; [c]Cognitive Science Center Amsterdam, University of Amsterdam, 1018 WS, Amsterdam, The Netherlands; and [d]Bernstein Center for Computational Neuroscience, Charité-Universitätsmedizin, 10115 Berlin, Germany

A number of studies have shown that pupil size increases transiently during effortful decisions. These decision-related changes in pupil size are mediated by central neuromodulatory systems, which also influence the internal state of brain regions engaged in decision making. It has been proposed that pupil-linked neuromodulatory systems are activated by the termination of decision processes, and, consequently, that these systems primarily affect the postdecisional brain state. Here, we present pupil results that run contrary to this proposal, suggesting an important intradecisional role. We measured pupil size while subjects formed protracted decisions about the presence or absence ("yes" vs. "no") of a visual contrast signal embedded in dynamic noise. Linear systems analysis revealed that the pupil was significantly driven by a sustained input throughout the course of the decision formation. This sustained component was larger than the transient component during the final choice (indicated by button press). The overall amplitude of pupil dilation during decision formation was bigger before yes than no choices, irrespective of the physical presence of the target signal. Remarkably, the magnitude of this pupil choice effect (yes > no) reflected the individual criterion: it was strongest in conservative subjects choosing yes against their bias. We conclude that the central neuromodulatory systems controlling pupil size are continuously engaged during decision formation in a way that reveals how the upcoming choice relates to the decision maker's attitude. Changes in brain state seem to interact with biased decision making in the face of uncertainty.

detection | neuromodulation | arousal | perceptual psychophysics

Changes in pupil size at constant luminance have long been used as a marker of central autonomic processes linked to cognition (1–4). Many studies over the past decades reported that the pupil dilates while subjects engage in demanding perceptual, cognitive, or economic decision tasks (1–3, 5–17). This decision-related pupil dilation has commonly been linked to the final choice terminating the decision process (6, 14, 16) and the consolidation of the committed decision (6, 16).

Changes in pupil size are also linked to changes in brain state. It has been proposed that the decision-related pupil dilation tracks the activity of certain neuromodulatory systems of the brainstem—in particular, the noradrenergic locus coeruleus (5, 7–9, 18) and, possibly, the cholinergic basal forebrain (19) systems. These neuromodulatory systems also activate briefly ("phasically") during perceptual decisions, such as visual target detection (5, 20–24), likely mediated via feedback connections from the prefrontal cortex (5, 25). The modulatory neurotransmitters released from the projections of these brainstem systems, in turn, shape the internal state of cortical networks, for instance, by boosting the gain of neural interactions (5, 7, 26). Thus, these brainstem systems might also shape decision computations in cortical networks—provided that they are activated already during decision formation. If so, these systems might affect the decision process, over and above shortening the time

to respond. For instance, they might govern the decision maker's ability to overcome his or her intrinsic bias.

Here, we addressed these issues noninvasively in humans by linking decision-related pupil dilation to the time course, outcome, and bias of a protracted perceptual decision process. Many perceptual decisions are not transient events but evolve gradually over several hundreds of milliseconds, due to the slow accumulation of noisy sensory information (27–33). Further, perceptual decisions are, like economic decisions (34), prone to strong biases that are not due to external asymmetries in the magnitude or probability of payoffs for certain choices. In particular "yes" vs. "no" detection decisions depend on the idiosyncratic (liberal or conservative) attitude of the decision maker with respect to saying "yes" or "no" (35, 36).

We thus measured pupil size in subjects performing a challenging yes–no visual contrast detection task at constant luminance (Fig. 1A). A general linear model (GLM) (37) allowed us to disentangle different temporal components of the neural input to the sluggish system controlling pupil size. This approach revealed that decision-related pupil dilation was not only driven by subjects' final choice and the concomitant motor response, but also by a (stronger) sustained component throughout the preceding decision process. Further, the dilation amplitude was bigger for yes than for no choices. This pupil choice effect was due to the conservative subjects who decided yes against their bias. Taken together, our findings point to an intricate interplay between changes in internal brain state and biased decision making in the face of uncertainty.

Significance

A number of studies reported that the pupil dilates (under constant illumination) during decision-making. Pupil dilation is also associated with the brain-wide release of modulatory neurotransmitters. It has remained unknown which specific elements of decision processes drive pupil dilation. Using a visual detection task, we here show that pupil dilation is primarily driven during, and not at the end of, a protracted decision. Further, pupil dilation differentiates between "yes" and "no" choices for conservative subjects deciding yes against their bias. Thus, pupil dilation reveals the content of the evolving decision and the decision maker's attitude. These findings have important implications for interpreting decision-related brain activity. They also point to a possible role of neuromodulation in interacting with decision biases.
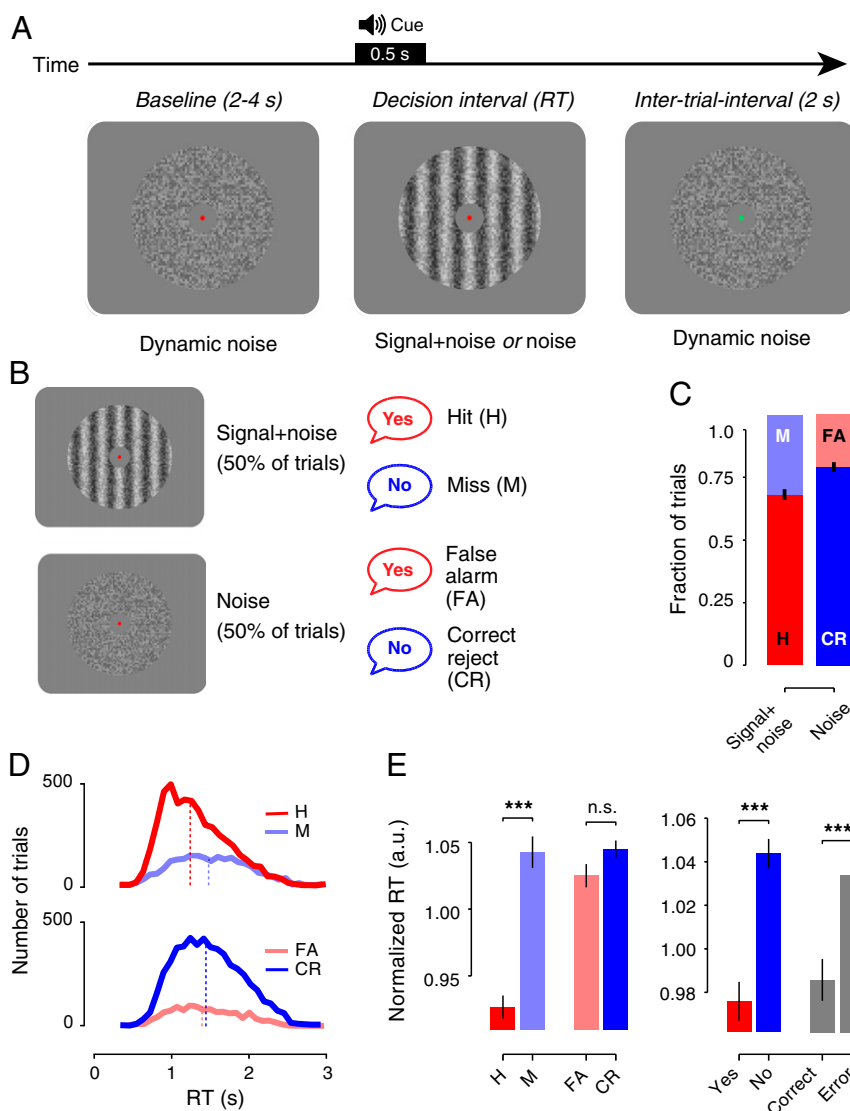
Fig. 1. Task and behavioral results. (*A*) Sequence of events during a single trial. Dynamic noise is continuously present in a circular aperture around fixation. During the decision interval (onset cued by a tone), the subject searches for a faint grating signal superimposed onto the noise and indicates the yes or no choice by button press. The signal is shown at high contrast for illustration purposes only. In the actual experiment, its contrast was titrated to each individual's detection threshold. (*B*) Stimulus types during the decision interval and possible choices of the subject, yielding the four trial categories of signal-detection theory. (*C*) Distribution of trial types, pooled across all subjects. (*D*) Reaction-time distributions for each trial type, pooled across all subjects. (*E*) Normalized reaction times, sorted by trial type and averaged across the group. RT, reaction time. Error bars, SEM.
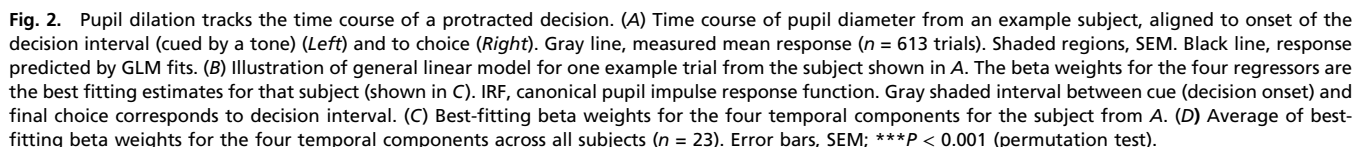
Results

Each trial of the detection task began with a baseline interval of variable duration, followed by an auditory cue that signaled the start of the subsequent decision interval (Fig. 1*A* and *Methods*). Low-contrast dynamic random noise was continuously present throughout the trial. On half of the trials, a low contrast vertical grating, the signal, was superimposed onto the noise during the decision interval (Fig. 1*B*). Subjects had to report a choice about the presence or absence of the signal (yes or no) by pressing one of two buttons. The signal contrast was adjusted individually such that each subject performed at about 75% correct (Fig. 1*C*). Based on the combination of physical stimulus and subjects' choices, we sorted the trials into four categories according to signal detection theory (35, 36) (Fig. 1*B*): hits (H, a yes choice on signal plus noise trials); misses (M, a no choice on signal plus noise trials); false alarms (FA, a yes choice on noise trials); correct rejects (CR, a no choice on noise trials).

Subjects produced long reaction times (Fig. 1*D*), consistent with a protracted decision process. When pooling trials across all participants, the median reaction times were longer than 1.5 s for all four trial categories. The median reaction times ranged between 1 and 2.44 s across individuals. Further, as commonly observed in yes–no choice tasks (38), reaction times were longer for no than for yes choices, and longer for incorrect than for correct choices (Fig. 1*E*).

Sustained Drive of Pupil Dilation Throughout a Protracted Decision Process. In all subjects, pupil diameter modulated during the decision interval (see Fig. 2*A* for an example subject; see Fig. S1 for all). These decision-related pupil responses were evident in all four trial categories and ranged from about 100 ms after the cue (a tone) signaling the onset of the decision interval to about 1,500 ms after the subjects' choice (Fig. 2 and Fig. S1).

In all subjects, the amplitude of decision-related pupil responses was strongly correlated to the baseline pupil diameter

Fig. 2. Pupil dilation tracks the time course of a protracted decision. (*A*) Time course of pupil diameter from an example subject, aligned to onset of the decision interval (cued by a tone) (*Left*) and to choice (*Right*). Gray line, measured mean response (*n* = 613 trials). Shaded regions, SEM. Black line, response predicted by GLM fits. (*B*) Illustration of general linear model for one example trial from the subject shown in *A*. The beta weights for the four regressors are the best fitting estimates for that subject (shown in *C*). IRF, canonical pupil impulse response function. Gray shaded interval between cue (decision onset) and final choice corresponds to decision interval. (*C*) Best-fitting beta weights for the four temporal components for the subject from *A*. (*D*) Average of best-fitting beta weights for the four temporal components across all subjects (*n* = 23). Error bars, SEM; ***P* < 0.001 (permutation test).

(Fig. S2). Although 23 subjects showed the previously reported (8, 39) decision-related pupil dilations with negative correlation to baseline diameter, the remaining 5 subjects showed the opposite: a decision-related pupil constriction with a positive correlation to baseline diameter (highlighted by rectangles in Figs. S1 and S2). We are not aware of any previous reports of such negative pupil responses during decision tasks at constant luminance. Therefore, we focus the subsequent report on the 23 subjects exhibiting the standard dilation response. However, the main results reported in this paper also hold for pupil modulations pooled across all 28 subjects (see below in the present section and *Pupil Dilation Reflects the Content of the Upcoming Choice and Individual Bias*).

We reasoned that the time course of decision-related neural input from the brainstem to the peripheral system controlling the pupil diameter could be modeled as the linear superposition of three elementary components (Fig. 2*B*): two transients, one at the beginning of the decision interval (cued by a tone), and another at the subjects' overt choice (button press); and a sustained component throughout the decision interval. For simplicity, we modeled the sustained component as a simple boxcar (i.e., constant amplitude throughout the decision interval), the duration of which varied from trial to trial (Fig. 2*B*), along with the reaction times (Fig. 1*D*). It is possible that persistent neural activity driving the pupil during the decision interval may have exhibited other shapes (e.g., gradual buildup, as observed in many decision-related brain regions) (see Fig. S4*A* and refs. 40–51); but the boxcar was the simplest model sufficient to test for the existence of a persistent neural input during decision formation. To determine the weight of each of these components in the pupil time series, we used a GLM with a pupil impulse response function adopted from ref. 37 (Fig. 2*B* and *Methods*). This model produced fits that were close to the measured pupil dilations during the decision interval (compare black and gray lines in Fig. 2*A*).

It has been proposed that decision-related brainstem activity (and, by inference, pupil dilation) is driven by the subject's final commitment to a choice (5, 6), or even the motor response used to report that choice (14). This scenario predicts a strong contribution of the transient at response, but not of the sustained component during decision formation. By contrast, we found that both of these components contributed significantly (see Fig. 2*C* for the example subject and Fig. 2*D* for the group). In fact, the biggest contribution was that of the sustained component, with beta weights of about 2.5 times those of the transient at the final choice. The transient elicited by the cue (i.e., decision onset) did not contribute significantly in the group average. The same pattern was evident in the whole group of 28 subjects (Fig. S3).

The conclusion that pupil dilation is driven during the decision formation (and more strongly than during the final behavioral choice) does not depend on the details of the GLM used here. We found the same qualitative pattern (in particular a statistically significant persistent component) for alternative models in which the boxcar function for the persistent input component during decision formation was substituted by a linear up ramp, akin to the neural buildup signals observed in decision-related brain regions (40–51) (or even a linear down ramp) (Fig. S4*A*). Further, we found that the contribution of the sustained (boxcar) component was significant across a wide range of the two free parameters of the pupil impulse response function (width and time-to-peak) (Fig. S4*B*) that we tested (Fig. S4*C*, *Center*). In sum, we conclude that the decision-related pupil dilation tracks the complete evolution of a perceptual decision and not merely the final choice.

Pupil Dilation Reflects the Content of the Upcoming Choice and Individual Bias. We wondered whether the decision-related pupil dilation might also contain information about the content of subjects' upcoming choice. Previous pupil dilation measurements in visual detection tasks found bigger dilations for hits than for misses (11, 13). This result may reflect two distinct scenarios.

First, pupil dilation is bigger during yes than no choices; second, pupil dilation is bigger during accurate than inaccurate choices. The signal-absent trials are critical to distinguish between these two scenarios: a signal that reflects the choice, but not its accuracy, should also be bigger for false alarms than correct rejects (52, 53). To test whether the pupil dilation reflects choice or accuracy, we collapsed the overall decision-related pupil modulation (mainly reflecting the sustained input) into a scalar amplitude measure per trial (*Methods*).

Pupil responses reflected subjects' yes vs. no choices in a categorical fashion, irrespective of whether the target was physically present and whether the choices were correct (Fig. 3). This pattern is clearly evident in the response-locked pupil time courses from the example subject in Fig. 3A, *Left*, who exhibited similar pupil responses during hits and false alarms, and smaller pupil responses during both misses and correct rejects. The same pattern (H > M and FA > CR) was evident (and statistically highly significant) in the overall pupil response amplitudes of the group as a whole (Fig. 3B). There was no evidence for a difference in pupil dilation during hits and false alarms ($P = 0.617$) and during misses and correct rejects ($P = 0.573$). Consequently, there was a highly significant amplitude difference between yes
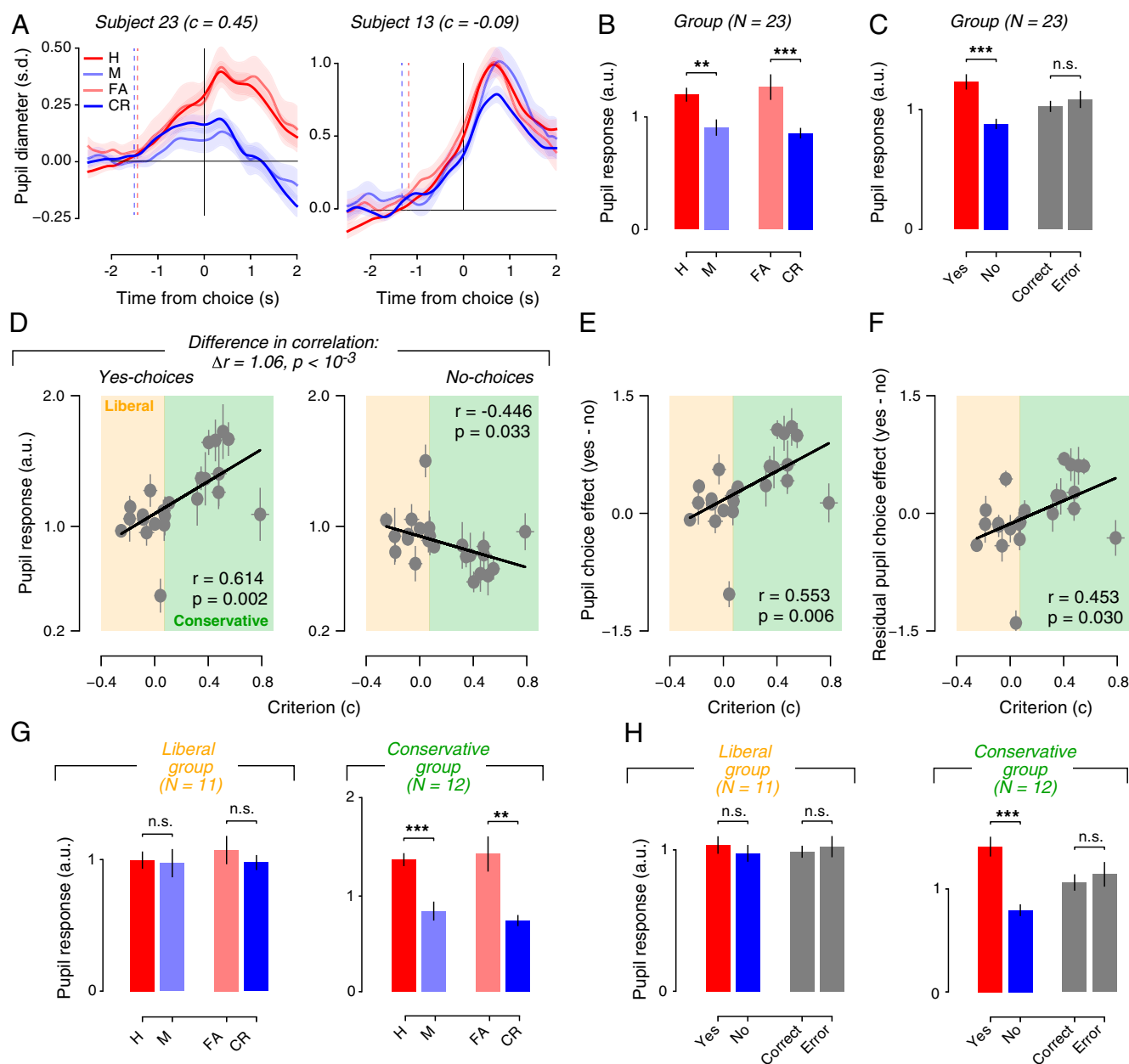

Fig. 3. Pupil dilation reflects the upcoming choice and intrinsic bias. (*A*) Time courses of pupil diameter (two example subjects) sorted by trial category and aligned to choice. Dashed lines, mean cue onset time (from choice) for "yes" (red) and "no" (blue) choices. Shaded regions, SEM. (*B* and *C*) Group average pupil response amplitudes, sorted by trial category (*B*) or by choice/correctness (*C*). Error bars, SEM; **$P < 0.01$; ***$P < 0.001$ (permutation test). (*D* and *E*) Pupil-response amplitude for both choices (*D*) or pupil choice effect (yes–no) (*E*), plotted against individual decision criteria. Each data point corresponds to one subject. Orange and green backgrounds indicate median split into liberal and conservative subgroups. Error bars, 60% confidence intervals (bootstrap). (*F*) As in *E*, but for residual pupil choice effect after removing the effect of reaction time. (*G* and *H*) As in *B* and *C*, but separately for liberal and conservative subgroups (median split). Error bars, SEM; **$P < 0.01$; ***$P < 0.001$ (permutation test).

and no choices, but not between correct choices and errors (Fig. 3C). Again, the same pattern was also true for the group of 28 subjects, including those with negative modulation amplitudes during decision formation (Fig. S5). In what follows, we refer to the difference in pupil response between yes and no choices as the pupil choice effect.

Remarkably, a large fraction of the individual differences in the pupil choice effect was explained by subjects' decision biases (Fig. 3 D–H), quantified in terms of criterion c of signal-detection theory (Methods). For example, a second, more liberal subject, shown in the right panel of Fig. 3A, despite strong decision-related pupil responses, hardly exhibited any difference between the four trial categories. In general, the more conservative the subject (i.e., the larger c), the bigger the pupil response amplitude during yes choices, and the smaller the pupil response amplitude during no choices (Fig. 3D). Consequently, the strength of the pupil choice effect depended on criterion (Fig. 3E).

In an alternative analysis, we split subjects into "liberal" and "conservative" subgroups based on the median criterion of the group (see colored backgrounds in Fig. 3 D–F). There was a highly significant interaction between the effects of choice (yes vs. no) and bias (conservative vs. liberal) on the pupil response (2-way repeated measures ANOVA $F_{1, 21} = 13,70$; $P = 0.0013$). The strong choice effect in the pupil was only evident in the conservative, but not the liberal, group (Fig. 3 G and H). This finding indicates that the overall choice effect shown in Fig. 3C reflects the conservative bias in the group of subjects as a whole. In sum, pupil dilation not only reflects the content of the upcoming choice, but also how that choice relates to the decision maker's bias.

Given the strong (negative, for the 23 subjects) trial-by-trial correlation between baseline pupil diameter and the pupil response during the decision interval (Fig. S2), we wondered whether the choice effect in the pupil dilation during decision formation may have been inherited from the preceding baseline interval. This scenario predicts that baseline pupil diameter should be larger for no than for yes choices—opposite to the choice effect found for the pupil response during the decision interval. In contrast to this prediction, we found that baseline pupil diameter also tended to be bigger before yes than no choices (Fig. S6 A and B). Further, the choice effects in the pupil responses during the decision interval and in the baseline pupil diameter were not significantly correlated (Fig. S6 C and D). Finally, the choice effect in the baseline pupil diameter was not correlated to criterion. Thus, the choice effects in baseline pupil diameter and pupil dilation during decision formation reflect separate processes.

Other Factors than Individual Bias Do Not Account for Pupil Choice Effect. The pupil choice effect was also not explained by differences in reaction times. Because the sluggish pupil impulse response (Fig. 2B) leads to accumulation of a sustained input, the pupil response is bound to increase with the duration of sustained inputs (up to about 1 s for the impulse response function estimated in ref. 37. As shown above, in our experiment, the pupil response was driven throughout the decision interval (Fig. 2). Thus, amplitude estimates will be larger when decision intervals are longer. Because subjects' reaction times were longer for no than for yes choices (Fig. 1E), the sluggishness of the pupil should have led to bigger pupil response amplitudes for no choices, opposite to the observed pupil choice effect. In sum, reaction times cannot account for the pupil choice effect, but instead may have led to an underestimation of the true effect size. Further, the dependence of the pupil choice effect on criterion remained significant after controlling for reaction time (Fig. 3F). As for the pupil choice effect, reaction time also depended on the interaction of choice and bias (two-way repeated measures ANOVA $F_{1, 21} = 8,55$; $P = 0.0081$) (Fig. S7). Because this inter-

action may have contributed to the criterion dependence of the pupil choice effect, we repeated the correlation between pupil choice effect and criterion after removing (by means of linear regression) the variance in the pupil choice effect explained by reaction time. The resulting partial correlation was also significant (Fig. 3F).

The pupil choice effect and its dependence on criterion were also not due to differences in eye movements (Fig. S8). Trials with saccades > 3 degrees of visual angle were excluded from the present analyses (Methods). However, we still detected smaller, residual gaze shifts (including microsaccades) in a substantial fraction (72%) of the trials. The amplitudes of the pupil responses during the decision interval exhibited a weak, and statistically significant, negative correlation to the number of these residual eye movements during the decision interval ($r = 0.08$; $P < 0.001$). However, the number of eye movements did not exhibit any choice effect (i.e., no significant difference between H and M and between FA and CR) (Fig. S8A), in contrast to the pupil response (Fig. 3B). Further, when repeating the correlation between pupil choice effect and criterion, after removing (by means of linear regression) the variance in the pupil choice effect accounted for by the number of eye movements, the resulting partial correlation remained highly significant (Fig. S8B).

Finally, the decision-related pupil dilation amplitude and the pupil choice effect also did not reflect the individual threshold contrast level (the inverse of subjects' perceptual sensitivity for the faint signals) (Fig. S9). Taken together, these control analyses underline the specificity of the pupil choice effect and its dependence on individual bias shown in Fig. 3.

Discussion

It has long been known that the pupil dilates during challenging mental tasks (1–3). More recent studies have linked pupil dilation to surprise about behaviorally relevant events (10, 12, 54), perceptual target detection (11, 13), and report of transitions between percepts in bistable perceptual phenomena (6, 14). Taken together, these findings establish that pupil dilation is a faithful reporter of the mental state of decision makers. Decision-related pupil dilation has commonly been linked to the final choice terminating the decision process (6, 14, 16). Consequently, the functional role of the underlying central brain processes has been attributed to consolidating decisions that have been made before (6, 16), rather than to shaping ongoing decisions as they evolve. One previous study of financial choice showed sustained pupil dilation throughout decision formation (17), but these authors did not dissociate the different components driving decision-related pupil dilation. Most importantly, decision-related pupil dilation has, so far, neither been linked to the specific contents of choices, nor to the bias of the decision maker.

By applying linear systems analysis techniques to pupil-dilation measurements during a protracted perceptual decision, we showed that pupil dilation (i) exhibits the strongest sustained component throughout decision formation, not at the end; (ii) predicts the content of the upcoming choice (yes > no); and (iii) reflects the decision maker's bias (boosted when conservative decision makers are about to respond yes against their bias). These results were highly specific and were neither explained by reaction times, fixational eye movements, nor individual perceptual sensitivity. Our results establish that pupil dilation faithfully tracks the formation of protracted perceptual decisions in a way that reflects both the evolving yes vs. no decision, and the decision maker's attitude toward that decision. It may prove fruitful to link pupil dilation to other elements of the decision process in future studies, such as the decision maker's level of confidence in his or her choice.

Our findings have some notable implications for interpreting neural correlates of perceptual decision making in visual cortex. First, the observed changes in pupil diameter imply that the

amount of light entering the eye during perceptul decisions fluctuates from trial to trial, depending on the content of the upcoming choice and the decision maker's bias. It will be important to determine how these changes in retinal illumination affect neural activity in visual cortex as measured with electrophysiology or functional magnetic resonance imaging. Second, given that several brainstem systems have widespread projections to visual cortex, our findings may (at least in part) account for the fact that widespread modulations of population activity in visual cortex also reflect subjects' "present" vs. "absent" choices in different perceptual tasks (53, 55–57). These activity modulations have commonly been interpreted in terms of decision-related feedback from downstream cortical regions. Our present results indicate that pupil-linked release of neuromodulators is a plausible alternative candidate source of these decision-related signals in visual cortex (58, 59).

The level of people's arousal fluctuates continuously on different time scales (5). These fluctuations reflect changes in global brain state (60, 61), governed by the release of neuromodulators from autonomic brainstem centers (5, 62). Traditionally, neuromodulators (and arousal) have been viewed as slow and nonspecific regulators of the overall behavioral state (61). Intermediate levels of arousal are commonly associated with the most accurate performance in sensory-motor choice tasks (5). However, it has become clear that neuromodulatory brainstem systems can be closely synchronized to rapid cognitive acts, such as decisions (5, 62, 63). Non–luminance-mediated pupil dilation seems to track the activity of these neuromodulatory brainstem centers, specifically the noradrenergic locus coeruleus (5). Under this assumption, our results suggest that pupil-linked brainstem systems receive diverse information from brain regions, including the cortical areas exhibiting sustained and/or ramping activity during decision formation (40–51), as well as (yet to be discovered) brain regions that encode the subjects' criterion.

Our current results also entail some notable differences to the results from direct measurements of locus coeruleus activity in animals. First, although the relationship between evolving decisions and the subject's bias was a major driving force behind the decision-related pupil dilation in our study, neural signatures of such a relationship have not yet been identified in the locus coeruleus. Second, the rapid nature of decision-related locus coeruleus activity observed in animals gave rise to the idea that this activity is primarily postdecisional (5). It is unclear whether these differences are due to differences between tasks, individuals, or species used, or whether they reflect genuine differences between pupil dilation and locus coeruleus activity. For example, the tasks used in previous animal physiology studies of locus coeruleus activity involved much faster decision processes (5) than the task used here. Future studies should determine whether the decision-related locus coeruleus activity also shows sustained activity corresponding to the pupil input during protracted decisions.

One model of locus coeruleus activity during decision making postulates an intradecisional drive of the locus coeruleus by surprise about decision-relevant events (64). It is conceivable that the bias-dependent choice component we found here is driven (at least in part) by surprise (10, 12) about the evolving yes decisions. The latter are, by definition, less frequent (thus, more surprising) for conservative than for liberal individuals. Importantly, regardless of the process driving the choice effect in the pupil, the fact that this effect occurs during decision formation suggests that the associated neuromodulator release may shape a decision process while it unfolds.

Our observations are consistent with the idea that pupil-linked neuromodulator release interacts with biased decision processing. Neuromodulators such as noradrenaline seem to boost the gain of neural interactions in the cortex (5, 7, 26). It is tempting to speculate that such a transient boost in gain during decision formation enables conservative subjects to overcome their bias

against responding "yes." Models of perceptual decision making help conceptualize this idea (29). In one specific scheme for yes vs. no choices, supported by neurophysiological data (43, 50, 65), two neural populations accumulate evidence for yes and no toward separate bounds, and compete via mutual inhibition (30, 43, 66). The yes population accumulates the sensory evidence for signal presence—i.e., neural activity in visual cortex (spontaneous activity in the case of false alarms) (53). The no population accumulates a "default input" (66). If there is an intrinsic asymmetry between these two populations (e.g., the yes population is larger or has stronger input gain), a global boost in neural gain will increase the rate of accumulation toward the yes choice. A conservative bias can be due to a shift in the starting point of the accumulation process (44)—in this case, away from the yes bound. Consequently, conservative subjects might require a stronger (pupil-linked) boost in gain for inputs from visual cortex to push the yes population toward the bound. Simultaneously monitoring brain activity and pupil dynamics during decision processing will allow for testing these ideas in future studies.

In conclusion, our findings indicate that the internal state of the brain changes each time one makes a decision, to an extent that reflects the content of the upcoming choice in relation to the decision maker's bias. Such decision-related changes in brain state may actively shape decisions as they unfold, perhaps by helping to overrule intrinsic biases. Tracking pupil size will be instrumental for unraveling how internal brain states interact with the brain mechanisms underlying perceptual decision making.

Methods

Subjects. The ethics committee of the Psychology Department of the University of Amsterdam approved the study. A total of 29 healthy subjects (14 females; age range, 18–38 y), including the authors, participated in the study. Twenty-six subjects were naive to the purpose of the study and participated after informed consent. These subjects were either paid for their participation or received research credit. All subjects had normal or corrected-to-normal vision. One subject was excluded from pupil analyses for breaking fixation on more than 30% of the trials, leaving 28 subjects in total.

Stimuli. Stimuli were presented on a 22-in LaCie Electron 22 blue IV gamma corrected screen with a spatial resolution of 768 × 1,024 pixels, run at a vertical refresh rate of 100 Hz. To minimize any effect of light on pupil diameter, the overall luminance of the display was held constant throughout the experiment. At all times, there was a dynamic noise pattern presented within this annulus, and the luminance across all pixels in this pattern deviated from the mean luminance symmetrically in both directions. This pedestal binary noise pattern of 5% contrast was refreshed on every frame. On "signal-plus-noise" trials, a sinusoidal grating with a vertical orientation (two cycles per degree) was superimposed on the noise for the period of the decision interval (Fig. 1). All stimuli were presented in a Gaussian annulus, with an average distance (± SD) to fixation of 4.8 ± 1.8 degrees (Fig. 1B). Throughout each run, the contrast of the grating (i.e., the signal strength) was fixed at each subject's 75% correct detection threshold level, as determined individually before the main experiment using the method of constant stimuli and discarding the effect of individual decision criteria (35, 36). Signal presence was randomly selected on each trial, under the constraint that it would occur on 50% of the trials within each block of 80 trials.

Task and Procedure. Subjects were instructed to form a decision about the presence or absence of the signal and report their choice by pressing one of two response buttons with the middle or index finger of their right hand, once they felt sufficiently certain (free response paradigm). The mapping between button press and choice (e.g., right key, yes; and left key, no) was counterbalanced across subjects. Each trial began with the central fixation dot turning red and consisted of the following consecutive intervals (Fig. 1A): (i) pretrial baseline interval (containing only noise); (ii) the decision interval [its onset was cued by a tone (beep of 500 ms duration), and it was terminated by the subject's response, or after a deadline (3 s in the first six subjects; 2.5 s in the remaining ones)]; and (iii) a fixed delay interval (containing only noise). Six of the 29 subjects were also prompted to rate their confidence and received auditory feedback after each choice. The present report focuses on pupil modulations during the decision interval, which were

qualitatively identical in both experimental protocols, leading us to pool the data together.

For the subjects reporting their confidence and receiving feedback, the trial timing was as follows: baseline interval uniformly distributed between 2.5 and 4.5 s; decision interval terminated after a maximum of 3 s; delay of 1.5 s, followed by confidence rating, followed by another delay of 1 s. These subjects performed between 12 and 17 sessions, yielding a total of 1,920–2,720 trials per subject (to afford within-subject statistics).

For the other 23 subjects, the trial timing was as follows: baseline interval uniformly distributed between 2 and 4 s; decision interval terminated after a maximum of 2.5 s; delay (intertrial interval) of 2 s. Self-paced pauses (during which subjects were allowed to make eye movements or blinks) were included between short blocks of three trials, during which they were informed about their overall performance on the last three trials. They performed between 6 and 10 sessions, yielding a total of 480–800 trials per subject (to afford the group-level statistics and correlations with individual bias).

Eye Data Acquisition. The diameter of the left eye's pupil was sampled at 1,000 Hz with an average spatial resolution of 15–30 min arc, using an EyeLink 1000 Desktop Mount (SR Research). Subjects were seated in a silent and dark room, with their head positioned on a chin rest, 50 cm in front of the computer screen.

Data Analysis. *Behavioral data.* Reaction time on every trial was computed as the time from decision onset (cued by tone) until the choice (button press). For group analyses, reaction times from each individual trial were normalized by each subject's median reaction time. We estimated decision bias in terms of the parametric criterion *c* of signal-detection theory, that is, by averaging the z-scores of hit and false-alarm rates and multiplying the result by −1 (36). *Preprocessing of pupil data.* Periods of blinks were detected using the manufacturer's standard algorithms with default settings. The remaining data analyses were performed using custom-made Python software. Blinks were removed by linear interpolation of values measured just before and after each identified blink (interpolation time window, from 100 ms before until 100 ms after blink). The first two trials from each run, as well as all trials with reaction times shorter than 250 ms, were excluded. Further, trials in which blinks or fixation errors occurred during the analysis epoch (from 500 ms before until 1.5 s after decision interval) were counted as omissions and were also excluded from further analysis of the pupil data. A trial was counted as fixation error when one or both of the following two criteria were met: (*i*) gaze deviations from fixation mark that were larger than half of the stimulus annulus (i.e., 7 degrees of visual angle); (*ii*) gaze deviations from fixation mark that were larger than the inner circle of the annulus (i.e., 3 degrees) and persisted for more than 10% of the trial time window. These errors were rare (median across subjects, 1.6% of trials). *GLM analysis of temporal input components.* The interpolated pupil time series were band-pass filtered (third order Butterworth, passband: 0.05–4 Hz) and z-scored for each run, based on the average and SD of pupil diameter across the whole time series. The GLM consisted of the following transient events (as individual 1s added onto a series of 0s): blinks, cue (onset of decision interval), and the choice (button press). Further, the GLM consisted of a sustained component during the decision interval, which was modeled as a boxcar function in the main analysis (Fig. 2). We normalized the boxcar regressor by dividing the height of the boxcar by the number of samples in that particular decision interval, such that this regressor had the same norm as the transient regressors. Thus, estimated beta weights were comparable between both sets of regressors. In different versions of the analysis, the sustained boxcar component was substituted by either a linear up or down ramp (Fig. S4A). Ramp regressors were also normalized (by half the number of samples in the decision interval), such that these regressors had the same norm as the transient regressors. Each regressor was then convolved with a canonical pupil impulse response function described in ref. 37:

$$h(t) = t^w e^{-t \cdot w / t_{\max}}, \qquad [1]$$

where *w* is the width and $t_{\max}$ the time-to-peak (ms) of the impulse response function (Fig. 2B and Fig. S4B). For the main analyses presented in Fig. 2 and Fig. S4A, we used the canonical values of these two parameters proposed by ref. 37, which were previously used to deconvolve pupil responses in the attentional blink (15): $w = 10.1$, $t_{\max} = 930$ ms. To verify that our conclusions did not depend on the choice of these specific parameters, we reran the GLM ("box"-model) for a wide range of combinations of *w* and $t_{\max}$ (Fig. S4C). The measured pupil time series and convolved regressors were baseline-corrected by subtracting, from each value in each time series, the average value from all pretrial baseline intervals (−0.5 to 0 s from onset of decision interval). The convolved and baseline-corrected regressors were horizontally concatenated into the complete design matrix. Multiple regression yielded the best-fitting beta weights for each regressor type (i.e., temporal component of the pupil response), separately for each subject. *Event-related analysis of pupil response amplitudes.* The interpolated pupil time series were low-pass filtered (third order Butterworth; cutoff, 4 Hz) and z-scored for each run, based on the average and SD of pupil diameter across the time window of the event-related pupil responses (0.5 s before to 1.5 s after the decision interval). We computed the baseline pupil diameter for each trial as the mean of all pretrial values in the window −0.5 to 0 s from onset of decision interval and subtracted this baseline value from the pupil time course on the same trial. We used linear projection of each single trial baseline-corrected pupil time course onto the average pupil time course of that subject, to obtain a scalar measure of the overall pupil modulation amplitude (positive or negative) for each trial:

$$A_i = \frac{R_i \cdot \overline{R}}{\left\| \overline{R} \right\|^2}, \qquad [2]$$

where R_i is the single trial pupil time course, *i* indexes trials, and $\overline{R}$ is the average pupil time course of a given subject. Pupil response amplitude measures were computed for the time window −1 s to 1.5 s from response, which consistently captured the peak of all subjects' pupil responses (Figs. 2 and 3 and Fig. S1) and encompassed, due to the delay, the sustained component and the transient at choice. *Statistical comparisons.* We used nonparametric permutation tests to test for significant differences between the beta weights of the GLM regressors as well as their difference to 0 (Fig. 2 and Figs. S3 and S4), and between the pupil measurements (Fig. 3 and Figs. S5 and S6), reaction times (Fig. 1 and Fig. S7), or eye movements (Fig. S8) from different trial categories. All these statistical comparisons were performed across subjects, using the mean per subject as observation. For each comparison, we randomly permuted the labels of the observations (e.g., the regressor label of the beta estimates; or the trial category label of pupil response amplitudes) and recalculated the difference between the two group means (10,000 permutations). The *P* value associated with the original difference between the means was given by the fraction of shuffles in which the original difference was exceeded by the difference between the means obtained for the shuffled data. When analyzing the correlation between the choice effect in pupil dilation and criterion, we also used a permutation procedure to test for differences between the correlation coefficients for yes and no choices (Fig. 3D). In this case, we permuted the condition labels (yes/no) of pairs of pupil dilation and criterion.

1. Hess EH, Polt JM (1964) Pupil size in relation to mental activity during simple problem-solving. *Science* 143(3611):1190–1192.
2. Kahneman D, Beatty J (1966) Pupil diameter and load on memory. *Science* 154(3756): 1583–1585.
3. Kahneman D, Beatty J, Pollack I (1967) Perceptual deficit during a mental task. *Science* 157(3785):218–219.
4. Beatty J (1982) Task-evoked pupillary responses, processing load, and the structure of processing resources. *Psychol Bull* 91(2):276–292.
5. Aston-Jones G, Cohen JD (2005) An integrative theory of locus coeruleus-norepinephrine function: Adaptive gain and optimal performance. *Annu Rev Neurosci* 28: 403–450.
6. Einhäuser W, Stout J, Koch C, Carter O (2008) Pupil dilation reflects perceptual selection and predicts subsequent stability in perceptual rivalry. *Proc Natl Acad Sci USA* 105(5):1704–1709.

7. Eldar E, Cohen JD, Niv Y (2013) The effects of neural gain on attention and learning. *Nat Neurosci* 16(8):1146–1153.
8. Gilzenrat MS, Nieuwenhuis S, Jepma M, Cohen JD (2010) Pupil diameter tracks changes in control state predicted by the adaptive gain theory of locus coeruleus function. *Cogn Affect Behav Neurosci* 10(2):252–269.
9. Jepma M, Nieuwenhuis S (2011) Pupil diameter predicts changes in the exploration-exploitation trade-off: Evidence for the adaptive gain theory. *J Cogn Neurosci* 23(7): 1587–1596.
10. Nassar MR, et al. (2012) Rational regulation of learning dynamics by pupil-linked arousal systems. *Nat Neurosci* 15(7):1040–1046.
11. Hakerem G, Sutton S (1966) Pupillary response at visual threshold. *Nature* 212(5061): 485–486.
12. Preuschoff K, 't Hart BM, Einhäuser W (2011) Pupil dilation signals surprise: Evidence for noradrenaline's role in decision making. *Front Neurosci* 5:115.

13. Privitera CM, Renninger LW, Carney T, Klein S, Aguilar M (2010) Pupil dilation during visual target detection. *J Vis* 10(10):3.

14. Hupé JM, Lamirel C, Lorenceau J (2009) Pupil dynamics during bistable motion perception. *J Vis* 9(7):10.

15. Wierda SM, van Rijn H, Taatgen NA, Martens S (2012) Pupil dilation deconvolution reveals the dynamics of attention at high temporal resolution. *Proc Natl Acad Sci USA* 109(22):8456–8460.

16. Einhauser W, Koch C, Carter OL (2010) Pupil dilation betrays the timing of decisions. *Front Hum Neurosci* 4:18.

17. Fiedler S, Glöckner A (2012) The dynamics of decision making in risky choice: An eye-tracking analysis. *Front Psychol* 3:335.

18. Nieuwenhuis S, De Geus EJ, Aston-Jones G (2010) The anatomical and functional relationship between the P3 and autonomic components of the orienting response. *Psychophysiology* 48(2):162–175.

19. Yu AJ (2012) Change is in the eye of the beholder. *Nat Neurosci* 15(7):933–935.

20. Sarter M, Parikh V (2005) Choline transporters, cholinergic transmission and cognition. *Nat Rev Neurosci* 6(1):48–56.

21. Parikh V, Kozak R, Martinez V, Sarter M (2007) Prefrontal acetylcholine release controls cue detection on multiple timescales. *Neuron* 56(1):141–154.

22. Rajkowski J, Majczynski H, Clayton E, Aston-Jones G (2004) Activation of monkey locus coeruleus neurons varies with difficulty and performance in a target detection task. *J Neurophysiol* 92(1):361–371.

23. Bouret S, Sara SJ (2005) Network reset: A simplified overarching theory of locus coeruleus noradrenaline function. *Trends Neurosci* 28(11):574–582.

24. Sara SJ (2009) The locus coeruleus and noradrenergic modulation of cognition. *Nat Rev Neurosci* 10(3):211–223.

25. Dayan P (2012) Twenty-five lessons from computational neuromodulation. *Neuron* 76(1):240–256.

26. Polack PO, Friedman J, Golshani P (2013) Cellular mechanisms of brain state-dependent gain modulation in visual cortex. *Nat Neurosci* 16(9):1331–1339.

27. Gold JI, Shadlen MN (2007) The neural basis of decision making. *Annu Rev Neurosci* 30:535–574.

28. Wang XJ (2008) Decision making in recurrent neuronal circuits. *Neuron* 60(2):215–234.

29. Bogacz R, Brown E, Moehlis J, Holmes P, Cohen JD (2006) The physics of optimal decision making: A formal analysis of models of performance in two-alternative forced-choice tasks. *Psychol Rev* 113(4):700–765.

30. Usher M, McClelland JL (2001) The time course of perceptual choice: The leaky, competing accumulator model. *Psychol Rev* 108(3):550–592.

31. Ossmy O, et al. (2013) The timescale of perceptual evidence integration can be adapted to the environment. *Curr Biol* 23(11):981–986.

32. Brunton BW, Botvinick MM, Brody CD (2013) Rats and humans can optimally accumulate evidence for decision-making. *Science* 340(6128):95–98.

33. Ratcliff R, McKoon G (2008) The diffusion decision model: Theory and data for two-choice decision tasks. *Neural Comput* 20(4):873–922.

34. Kahneman D (2003) Maps of bounded rationality: A perspective on intuitive judgement and choice. *Les Prix Nobel 2002*, ed Frangsmyr T (Almquist & Wiksel International, Stockholm).

35. Green DM, Swets JA (1966) *Signal Detection Theory and Psychophysics* (Wiley, New York).

36. Macmillan NA, Creelman CD (2005) *Detection Theory: A User's Guide* (Lawrence Erlbaum Associates, Inc., Mahwah, NJ).

37. Hoeks B, Levelt WJM (1993) Pupillary dilation as a measure of attention: A quantitative systems analysis. *Behav Res Methods Instrum Comput* 25(1):16–26.

38. Wolfe JM, Palmer EM, Horowitz TS (2010) Reaction time distributions constrain models of visual search. *Vision Res* 50(14):1304–1311.

39. Murphy PR, Robertson IH, Balsters JH, O'connell RG (2011) Pupillometry and P3 index the locus coeruleus-noradrenergic arousal function in humans. *Psychophysiology* 48(11):1532–1543.

40. Shadlen MN, Newsome WT (2001) Neural basis of a perceptual decision in the parietal cortex (area LIP) of the rhesus monkey. *J Neurophysiol* 86(4):1916–1936.

41. Hanes DP, Schall JD (1996) Neural control of voluntary movement initiation. *Science* 274(5286):427–430.

42. Philiastides MG, Ratcliff R, Sajda P (2006) Neural representation of task difficulty and decision making during perceptual categorization: A timing diagram. *J Neurosci* 26(35):8965–8975.

43. Donner TH, Siegel M, Fries P, Engel AK (2009) Buildup of choice-predictive activity in human motor cortex during perceptual decision making. *Curr Biol* 19(18):1581–1585.

44. de Lange FP, Rahnev DA, Donner TH, Lau H (2013) Prestimulus oscillatory activity over motor cortex reflects perceptual expectations. *J Neurosci* 33(4):1400–1410.

45. O'Connell RG, Dockree PM, Kelly SP (2012) A supramodal accumulation-to-bound signal that determines perceptual decisions in humans. *Nat Neurosci* 15(12):1729–1735.

46. Wyart V, de Gardelle V, Scholl J, Summerfield C (2012) Rhythmic fluctuations in evidence accumulation during decision making in the human brain. *Neuron* 76(4):847–858.

47. Kim JN, Shadlen MN (1999) Neural correlates of a decision in the dorsolateral prefrontal cortex of the macaque. *Nat Neurosci* 2(2):176–185.

48. Gold JI, Shadlen MN (2000) Representation of a perceptual decision in developing oculomotor commands. *Nature* 404(6776):390–394.

49. Haegens S, et al. (2011) Beta oscillations in the monkey sensorimotor network reflect somatosensory decision making. *Proc Natl Acad Sci USA* 108(26):10708–10713.

50. de Lafuente V, Romo R (2006) Neural correlate of subjective sensory experience gradually builds up across cortical areas. *Proc Natl Acad Sci USA* 103(39):14266–14271.

51. Siegel M, Engel AK, Donner TH (2011) Cortical network dynamics of perceptual decision-making in the human brain. *Front Hum Neurosci* 5:21.

52. Donner TH, et al. (2007) Population activity in the human dorsal pathway predicts the accuracy of visual motion detection. *J Neurophysiol* 98(1):345–359.

53. Ress D, Heeger DJ (2003) Neuronal correlates of perception in early visual cortex. *Nat Neurosci* 6(4):414–420.

54. Naber M, Frässle S, Rutishauser U, Einhäuser W (2013) Pupil size signals novelty and predicts later retrieval success for declarative memories of natural scenes. *J Vis* 13(2):11.

55. Donner TH, Sagi D, Bonneh YS, Heeger DJ (2008) Opposite neural signatures of motion-induced blindness in human dorsal and ventral visual cortex. *J Neurosci* 28(41):10298–10310.

56. Moradi F, Hipp C, Koch C (2007) Activity in the visual cortex is modulated by top-down attention locked to reaction time. *J Cogn Neurosci* 19(2):331–340.

57. Kloosterman NA, Hillebrand A, van Dijk B, Lamme VAF, Donner TH (2012) Amplitude of oscillatory activity in human visual cortex predicts duration of bistable perceptual states. Program no. 96.21/XX4. 2012. *Neuroscience Meeting Planner* (Society for Neuroscience, New Orleans, LA). Available at http://www.abstractsonline.com/Plan/ViewAbstract.aspx?sKey=b638a47f-b6b7-439c-8cf7-382a9198296d&cKey=7e4eb1c6-379b-41f7-87d7-8d9eb9df1fd2&mKey=%7b70007181-01C9-4DE9-A0A2-EEBFA14CD9F1%7d. Accessed October 1, 2012.

58. Jack AI, Shulman GL, Snyder AZ, McAvoy M, Corbetta M (2006) Separate modulations of human V1 associated with spatial attention and task structure. *Neuron* 51(1):135–147.

59. Sirotin YB, Das A (2009) Anticipatory haemodynamic signals in sensory cortex not predicted by local neuronal activity. *Nature* 457(7228):475–479.

60. Palva JM, et al. (2013) Neuronal long-range temporal correlations and avalanche dynamics are correlated with behavioral scaling laws. *Proc Natl Acad Sci USA* 110(9):3585–3590.

61. Steriade M (2000) Corticothalamic resonance, states of vigilance and mentation. *Neuroscience* 101(2):243–276.

62. Sarter M, Parikh V, Howe WM (2009) Phasic acetylcholine release and the volume transmission hypothesis: Time to move on. *Nat Rev Neurosci* 10(5):383–390.

63. de Lafuente V, Romo R (2011) Dopamine neurons code subjective sensory experience and uncertainty of perceptual decisions. *Proc Natl Acad Sci USA* 108(49):19767–19771.

64. Dayan P, Yu AJ (2006) Phasic norepinephrine: A neural interrupt signal for unexpected events. *Network* 17(4):335–350.

65. Merten K, Nieder A (2012) Active encoding of decisions about stimulus absence in primate prefrontal cortex neurons. *Proc Natl Acad Sci USA* 109(16):6289–6294.

66. Deco G, Pérez-Sanagustín M, de Lafuente V, Romo R (2007) Perceptual detection as a dynamical bistability phenomenon: A neurocomputational correlate of sensation. *Proc Natl Acad Sci USA* 104(50):20073–20077.

Supporting Information

de Gee et al. 10.1073/pnas.1317557111
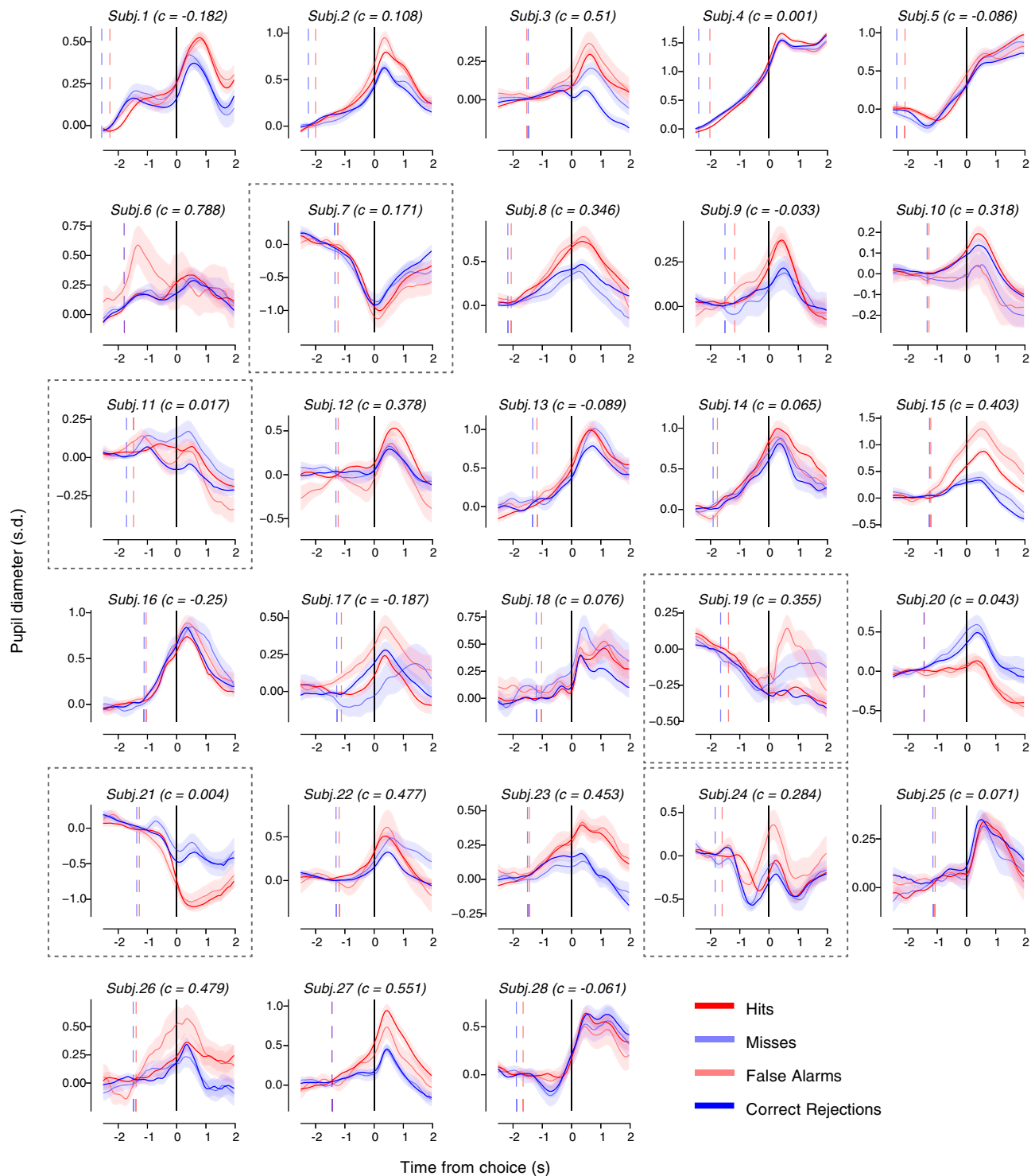
Fig. S1. Modulations of pupil diameter during the decision interval. Mean time courses of pupil diameter from all subjects, sorted by trial types and aligned to choice. Shaded regions, SEM. Rectangles highlight subjects with negative overall pupil responses during decision interval (see also Fig. S2), computed by averaging pupil responses across all four trial types and summing up the samples of the resulting average response in the time window (−1 to 1.5 s from response). The five highlighted subjects had a negative sum.

Fig. S2. Correlation between pupil response and baseline pupil diameter. Single-trial pupil response amplitude per subject plotted against single-trial baseline pupil diameter. Dashed rectangles indicate subjects with an inverse effect (pupil constriction) during the decision interval (see also Fig. S1). These subjects show a positive correlation to baseline diameter whereas all other subjects (who have a pupil dilation response) show a negative correlation.

Fig. S3. Pupil dilation tracks the time course of a protracted decision ($n = 28$). Average of best-fitting beta weights for the four temporal components across all subjects. Error bars, SEM. ***$P < 0.001$. Because five subjects showed an inverse effect (pupil constriction) during the decision interval (see Figs. S1 and S2), we here quantified only the overall modulation, regardless of sign. To take this observation into account, we focused this control analysis on the comparison between the temporal components (rather than also comparing each component against 0). To this end, we took the absolute value of the single-subject beta weights for each component, before comparing them between components. Note that the comparison against 0 becomes meaningless in this situation.

Fig. S4. Sustained input during decision does not depend on specifics of GLM. (*A*) Alternative models of the persistent input component. Format as in Fig. 1. Model 2 consists of a linear up ramp instead of boxcar; model 3 consists of a linear down ramp instead of boxcar. The transient regressors are identical for all models. Both models (fitted separately) yield a robust and statistically significant component during decision formation that is larger than the transient at the time of behavioral choice. (*B*) Shapes of the pupil IRFs with different parameter combinations used for *C*, with the standard parameters (used for Fig. 2 and *A*) plotted in black. The width and time-to-peak parameters are varied across the following range: w, 4, 6, 8, 10.1 (canonical), 12, 14, 16; t_{max}, 500, 650, 800, 930 (canonical), 1,100, 1,250, 1,400. (*C*) Matrix of average beta values for choice and box components, as well as their difference, based on the IRF parameter combinations shown in *B*. Color-coded cells correspond to significant beta values ($P < 0.05$ permutation test).
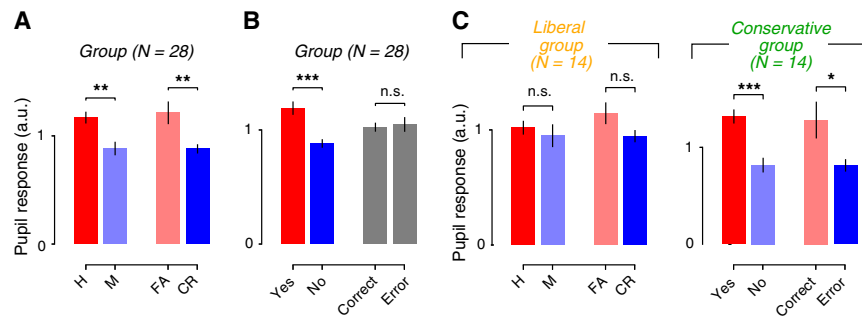
Fig. S5. Pupil dilation reflects the upcoming choice and intrinsic bias (n = 28). (*A*) Pupil response amplitudes, sorted by trial type and averaged across all subjects. (*B*) Pupil response amplitudes, sorted by choice or by correctness and averaged across the group. (*C*) As in *A*, but separately for liberal and conservative subjects (median split). Error bars, SEM. **P < 0.01; ***P < 0.001. Note that our linear projection procedure (used to compute single-trial pupil response amplitudes; see *Methods*) quantifies the overall modulation amplitude, with respect to each subject's mean response, irrespective of the polarity of the response. In other words, even for those subjects with pupil constriction during the decision interval (i.e., negative polarity), the linear projection yields positive amplitude estimates for all negative single-trial responses (the bigger, the more negative the response). The linear projection yields negative amplitude estimates only for single-trial responses that have opposite sign to the mean response.
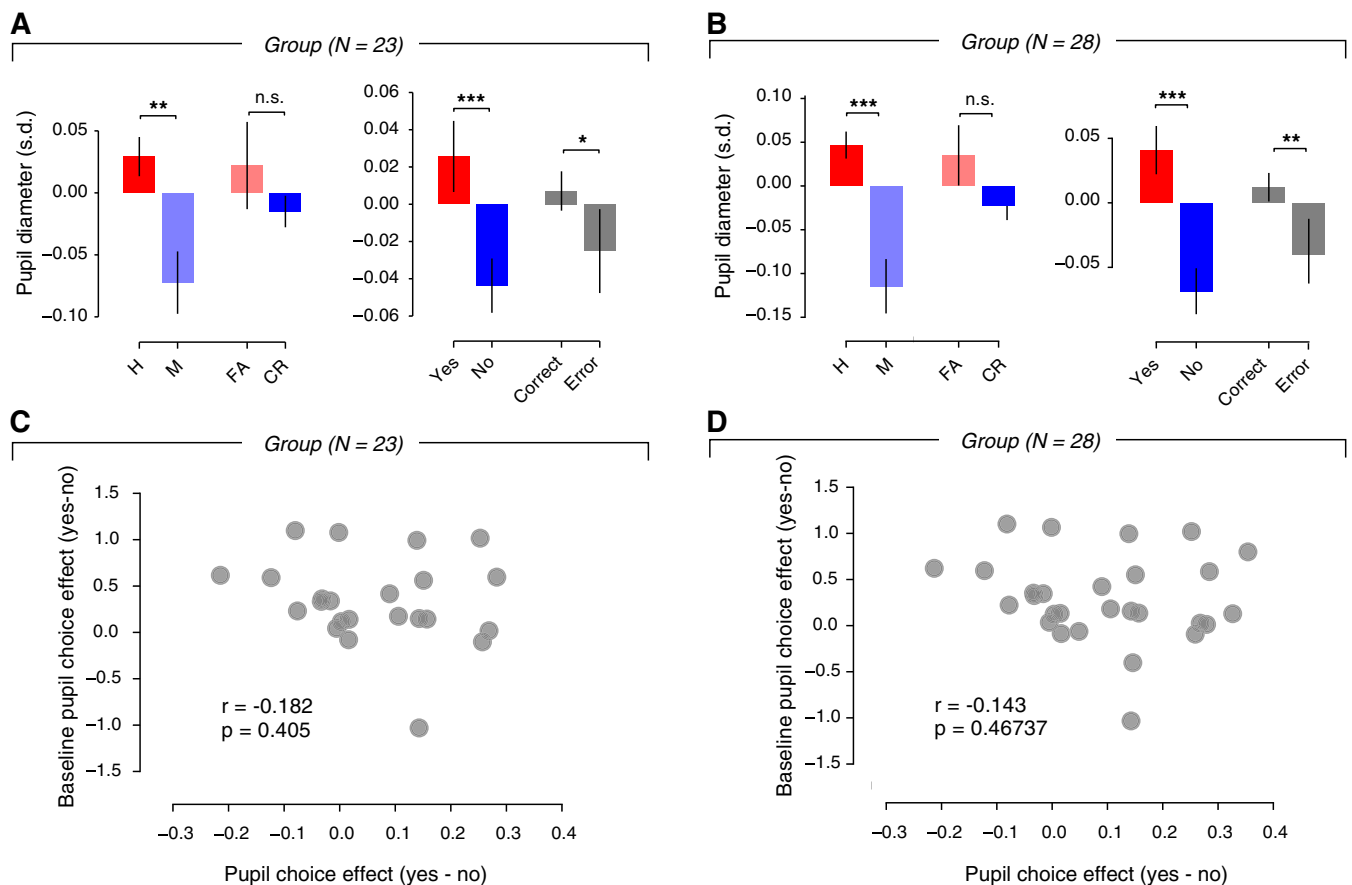

Fig. S6. Choice effects in baseline pupil diameter is decoupled from choice effect in pupil response during decision interval. (*A*) Baseline pupil diameter, sorted by trial type (*Left*), and sorted by choice or by correctness (*Right*), and averaged across the group (n = 23). (*B*) Baseline pupil diameter, sorted by trial type (*Left*), and sorted by choice or by correctness (*Right*), and averaged across the group (n = 28). (*C*) Mean choice effect (yes–no difference) in baseline pupil diameter per subject plotted against mean choice effect in pupil response (n = 23). (*D*) Mean choice effect (yes–no difference) in baseline pupil diameter per subject plotted against mean choice effect in pupil response (n = 28). Error bars, SEM. *P < 0.05; **P < 0.01; ***P < 0.001. Baseline pupil diameter was quantified as follows. The interpolated pupil time series were low pass-filtered (cutoff, 4 Hz) and z-scored for each run, based on the average and SD of pupil diameter across the time window of the baseline pupil diameter (−0.5 to 0 s from onset of decision interval). We computed the baseline pupil diameter for each trial as the mean of all pretrial values in the window −0.5 to 0 s from onset of decision interval. This procedure forced average baseline pupil diameter (across all trials) per subject to be 0.
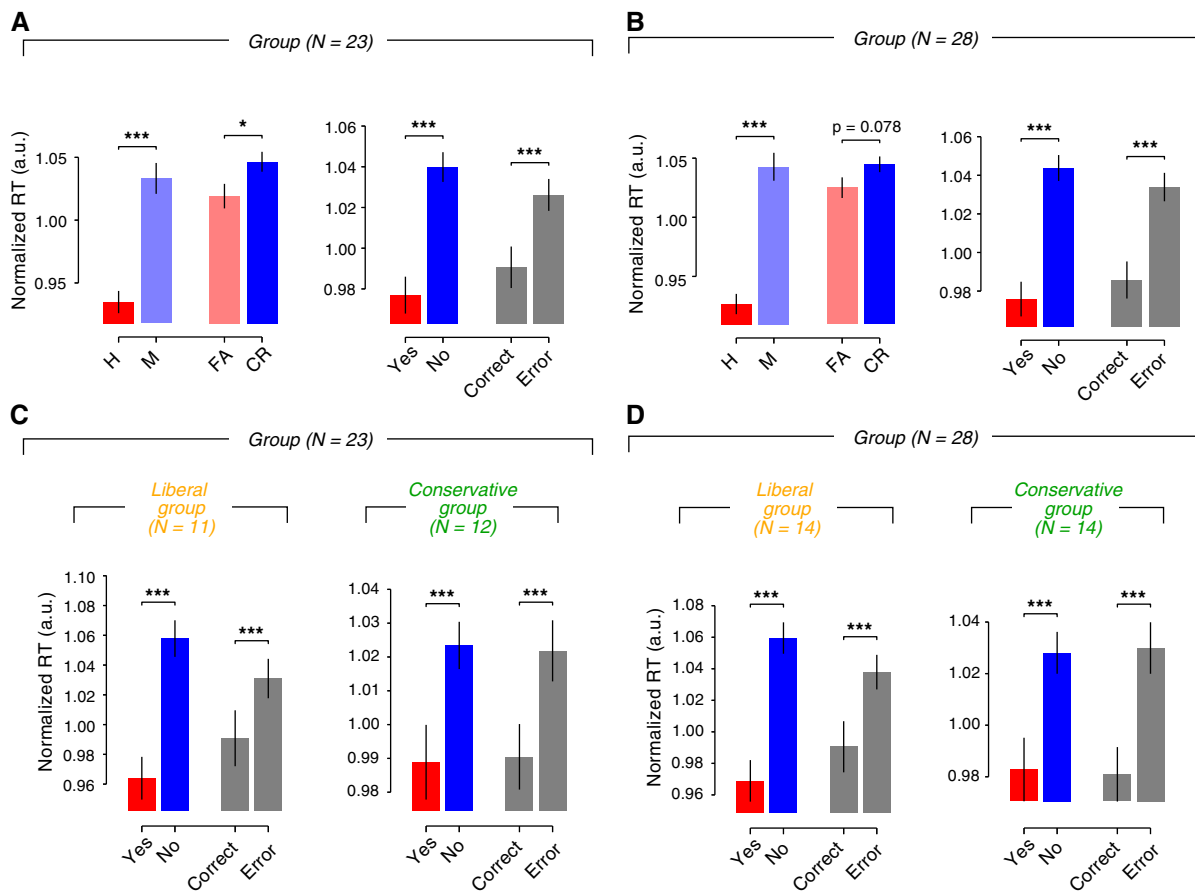
Fig. S7. Reaction times as a function of choice and decision bias. (*A*) Normalized reaction times, sorted by trial type (*Left*) or by choice content and accuracy (*Right*), averaged across all subjects with positive pupil response (n = 23). (*B*) Same as in *A*, but for the whole group (n = 28). (*C*) As in *A*, but separately for liberal and conservative subjects (median split). (*D*) As in *C*, but for the whole group (n = 28). Error bars, SEM. *P < 0.05; ***P < 0.001.
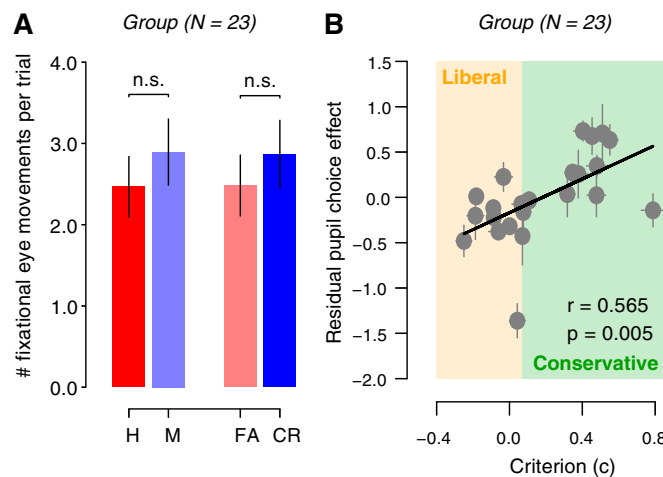

Fig. S8. Eye movements are unrelated to pupil choice effect. (*A*) The number of residual eye movements after excluding trials with large fixation errors (see *Methods*) during the decision interval did not differ significantly between yes and no choices. Error bars, SEM. (*B*) Correlation between pupil choice effect and criterion after removing (by means of linear regression) the variance in the pupil choice effect explained by the number of eye movements. The resulting partial correlation is highly significant. Error bars, 60% confidence intervals (bootstrap).
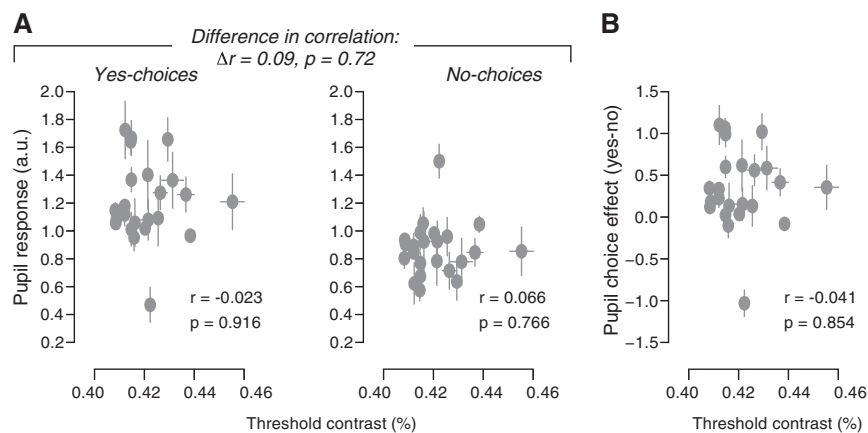
Fig. S9. Pupil choice effect is not correlated to threshold contrast value. (*A*) Average pupil response amplitude per subject against subjects' individual threshold contrast. (*Left*) Yes choices. (*Right*) No choices. Difference in correlation is assessed by means of permutation test. (*B*) As in *A*, but for difference of average pupil response amplitudes for yes and no choices (pupil choice effect) per subject. Error bars, 60% confidence intervals (bootstrap).